Validity of linear analysis in early-stage spinodal decomposition of a polymer mixture

ARTICLE *in* THE JOURNAL OF CHEMICAL PHYSICS · AUGUST 2000

Impact Factor: 2.95 · DOI: 10.1063/1.1287272

3 AUTHORS, INCLUDING:

Hiroshi Jinnai
Tohoku University
234 PUBLICATIONS **4,233** CITATIONS
SEE PROFILE

Takeji Hashimoto
Kyoto University
516 PUBLICATIONS **16,964** CITATIONS
SEE PROFILE

Validity of linear analysis in early-stage spinodal decomposition of a polymer mixture

Masaki Hayashi, Hiroshi Jinnai,[a] and Takeji Hashimoto[b]
Department of Polymer Chemistry, Graduate School of Engineering, Kyoto University, Kyoto 606-8501, Japan

(Received 13 January 2000; accepted 26 May 2000)

A two-step phase separation was imposed to a binary mixture of deuterated polybutadiene and protonated polyisoprene with nearly critical composition in the following way: the system was first subjected to phase separation via spinodal decomposition (SD) so that the system developed coexisting two phases characteristics of the late stage of SD (the first-step phase separation). It was then brought into a deeper quench so that both two phases again fell into spinodal region and hence further SD took place within each phase (the second-step phase separation at T_2). In the very early stage after this second-step phase separation, the two-phase structure developed in the first-step phase separation was almost unchanged with time, but the composition fluctuation was newly developed within each phase, giving rise to an excess light scattering (LS) at large scattering vectors. The very early stage in this second-step phase separation process was studied by time-resolved LS. We found that the early-stage SD after the second-step phase separation at T_2 can be well described by the linearized theory of SD. However the characteristic parameters, especially the collective diffusivity, obtained from the linear analysis, were different from those obtained by the single-step SD at T_2 for the corresponding single-phase mixtures. The results unveil an intriguing effect of initial structure or space confinement on early stage SD, reflecting an intrinsically nonlinear phenomenon. © *2000 American Institute of Physics.*
[S0021-9606(00)51732-2]

I. INTRODUCTION

Time evolution of self-assembling structures of molecules in binary mixtures via spinodal decomposition (SD) is one of nonlinear and nonequlibrium phenomena.[1–3] It is important to unveil various characteristics associated with the nonlinear time evolution process. In order to unveil them, we have been investigating a particular phase separation process designated as a ''two-step phase separation'' process by using a model polymer mixture of perdeuterated polybutadiene (dPB) and protonated polyisoprene (hPI) approximately having critical composition.[4,5]

Since the objectives and merits of the two-step phase separation process were well described in our previous papers,[4,5] they will not be repeated here. However we shall briefly describe below the process and the results obtained so far for readers who may be interested in this part only. The process involves first isothermal phase separation via SD at temperature T_1 into a late stage SD for various time interval, t_0, by quenching the mixture from a single phase state at temperature T_0 inside a spinodal region to temperature T_1 (see Fig. 1 later). In the end of the first-step process we obtained well defined initial structures composed of coexisting two phases with various characteristic sizes $\Lambda_{m,1}$ for the second-step phase separation process triggered at time t_0 by a temperature jump (T-jump) from T_1 to T_2. The second-step phase separation process was designed in such a way that the two coexisting phases developed in the first-step are again brought into spinodal region and hence subjected to thermodynamic instability. We have been exploring nonlinear pathways that the system takes to achieve a new equilibrium at T_2 during the course of the second-step phase separation process under various initial structures with the sizes $\Lambda_{m,1}(t_0)$ set up in the first-step process.

We proposed a new scaling idea[4] for the two-step process which takes into account a change in spatio-temporal scale induced by the temperature change from T_1 to T_2. The new scaling allows to predict the nonlinear pathways of the *large domains* in real time scale after the second-step.

We found that the pathways depend on the initial structures.[5] When the size of the initial structure $[\Lambda_{m,1}(t_0)]$ is larger than the characteristic size $\Lambda_{m,0}$ for the composition fluctuations developed in the early stage SD at T_2, small domains are evolved within the domains developed in the first-step (designated as ''large domains''). On the other hand when $\Lambda_{m,1}(t_0) \leqslant \Lambda_{m,0}$, small domains are not evolved but rather only the large domains further grow at a different rate.[5] In the case when $\Lambda_{m,1}(t_0) > \Lambda_{m,0}$, the time evolution of the small domains was found to be intricately coupled with that of large domains. The pathways involved were found to be classified into the following three stages,[2] similarly to a single-step SD induced by quenching from T_0. Regime I where the small domains evolve and grow to result in amplitude of the composition fluctuations of the system as a whole changing from that at T_1 toward the new equilibrium

[a]Present address: Department of Polymer Science and Engineering, Kyoto Institute of Technology, Matsugasaki, Sakyo-ku, Kyoto 606-8585, Japan.
[b]Author to whom correspondence should be addressed.

TABLE I. Polymer characteristics.

Polymer	$M_n \times 10^{-4}$ [a]	M_w/M_n [a]	N_n [b]
dPB	6.10	1.07	950
hPI	14.1	1.04	2000

[a]Determined by size exclusion chromatography equipped with light scattering.
[b]Number-average degree of polymerization.

at T_2; Regime II where the amplitude reached equilibrium value at T_2, and both small domains and large domains grow with dynamical self-similarity, interestingly enough with a single time-dependent length parameter, i.e., with the same dynamical scaling law; Regime III where the small domains annihilate and are absorbed into the large domains.

In this work we focused on very early stage of phase separation after onset of the second-step process in the criterion satisfying $\Lambda_{m,1}(t_0) > \Lambda_{m,0}$, where the coexisting large domains with equilibrium compositions at T_1 become thermodynamically unstable at T_2 and undergo SD to result in formation of small domains. In this stage, size of the large domains is essentially fixed, and hence the large domains are considered to provide a confined space for the new composition fluctuations developed in the very early-stage of the SD process at T_2. We are interested in exploring whether or not the early stage SD process after onset of the second-step phase separation is described by the linearized theory of SD,[6,7] and whether or not this special space confinement effect affects the early stage dynamics. Despite the physical significance from a viewpoint of nonlinear dynamics, this confinement effect on the early stage dynamics has neither been explored yet in general nor by the previous pioneering experiments on two-step phase separation by Okada *et al.*,[8] Tanaka,[9] and Tao *et al.*[10] This effect has been left unexplored in our previous works[4,5] as well.

II. EXPERIMENT

The polymers used in this study are summarized in Table I. Both dPB and hPI used in the present study were synthesized by living anionic polymerization. In the present study, three binary mixtures of dPB/hPI with the different volume fractions of dPB, $\phi_{\mathrm{dPB}} = 0.502$, 0.752, and 0.586, were used as shown in Table II. The respective dPB/hPI mixtures were dissolved in toluene in such a way that total polymer concentration was equal to 5%. Then the solution was cast into thin films of thickness ≈ 0.2 mm. The films were dried until constant weight was attained. The as-cast

TABLE II. Polymer blends studied in this work and the experimental condition.

Mixture code	dPB/hPI (vol %/vol %)	Thermal history
Two-step SD process		
C	58.6/41.4	$T_0 \rightarrow T_1(t_0 = 2865\ \mathrm{min}) \rightarrow T_2$
Single-step SD process		
A	50.2/49.8	$T_0 \rightarrow T_2$
B	75.2/24.8	$T_0 \rightarrow T_2$

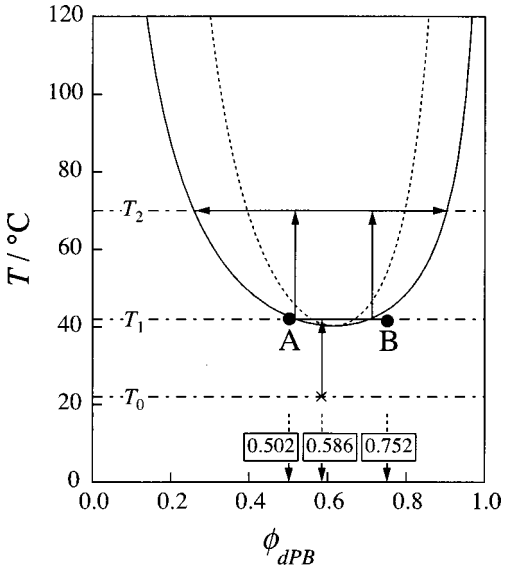

FIG. 1. Phase diagram of a binary mixture of dPB/hPI. The solid and dotted curves correspond, respectively, to the binodal and spinodal line calculated as described in Ref. 4. The filled circles A and B correspond to the equilibrium compositions of coexisting phases at T_1 obtained by cloud point measurements, the respective compositions of which are written in the figure together with that of mixture C. The two-step temperature jump was performed with mixture C according to the scheme indicated by arrows.

film specimens thus obtained were stacked on a cover glass with 0.2 mm thickness Teflon® spacer, degassed under vacuum at room temperature for about 12 h, and covered by another cover glass. The assembly was then put in an aluminum cell for light scattering (LS). The cell was placed into a temperature enclosure controlled to a phase separation temperature. Scattering profiles were taken as a function of scattering angle (in the medium), θ, by using the time-resolved LS (TRLS) apparatus[11] equipped with a He–Ne laser with a wavelength in vacuum, λ, of 632.8 nm as a light source.

Here we designate the binary mixture with $\phi_{\mathrm{dPB}} = 0.502$ as mixture ''A,'' that with $\phi_{\mathrm{dPB}} = 0.752$ as mixture ''B,'' and that with $\phi_{\mathrm{dPB}} = 0.586$ as mixture ''C,'' respectively. The binary mixture of dPB/hPI has a critical composition, $\phi_{c,\mathrm{dPB}} = 0.616$ (and $\phi_{c,\mathrm{hPI}} = 0.384$), predicted by the Flory–Huggins theory[12] and has a lower critical temperature (LCST) type phase diagram with a critical temperature of ≈ 36 °C as shown in Fig. 1 and as described elsewhere.[4] Note that the filled circles A and B in Fig. 1 indicate the equilibrium compositions of coexisting phases at T_1, which were experimentally obtained by cloud-point measurements with the LS method.[4] Thus, the three blends at room temperature are in the single-phase region at thermal equilibrium. We should note that the compositions of mixtures A and B nearly correspond to the equilibrium compositions of the two coexisting phases at 42 °C (designated hereafter as temperature T_1), respectively. The TRLS experiments were performed in the following way.

Mixture C, having a near critical composition, was used in order to perform the two-step phase separation. The T-jump conducted here are indicated by arrows in Fig. 1. The first-step SD was carried out by inserting the sample of mixture C at room temperature (a single-phase state and desig-

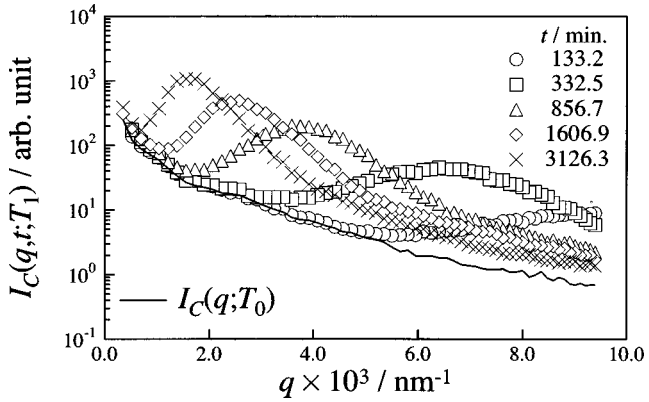

FIG. 2. Time evolution of the light scattering profile in the single-step isothermal SD process at T_1 for mixture C. The solid line, $I_C(q;T_0)$, corresponds to the LS profile obtained in the single-phase state at T_0 (room temperature).

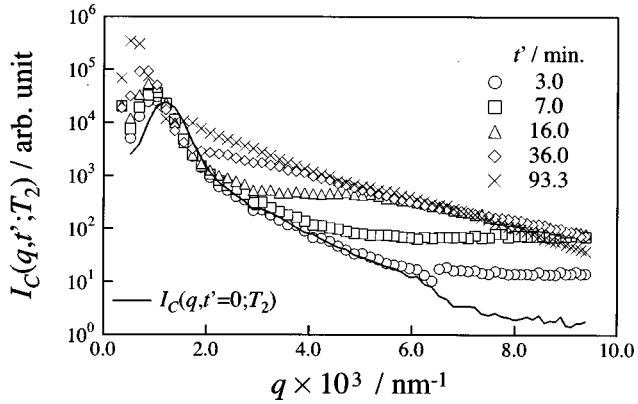

FIG. 3. Time evolution of the light scattering profile in the second-step phase separation process at T_2 for mixture C. t' was defined as the time elapsed after the onset of the second-step temperature jump. The solid line, $I_C(q,t'=0;T_2)$, corresponds to the LS profile obtained immediately before the second-step T-jump. The peak of the scattering intensity at $t'=0$ existed at $q \equiv q_{m,1}(t'=0) = 1.19 \times 10^{-3}$ nm^{-1}, which corresponds to the wavelength of the dominant mode of the composition fluctuations, 5.28 μm.

nated hereafter as temperature T_0) into a copper block controlled at T_1. The blend specimens were annealed at T_1 for t_0 minutes ($t_0 = 2865$) so that the system reached the late stage of SD (see Sec. III A), where time t is defined as the time spent after onset of the first-step SD at T_1, and t_0 is the time when the second-step phase separation was conducted. The second-step phase separation was imposed on the system by transferring the phase-separated sample of mixture C at T_1 for t_0 into another copper block controlled at 70 °C (designated as hereafter temperature T_2) that was installed in the LS apparatus. In addition to the two-step phase separation process, the single-step isothermal SD process at T_1 was also conducted and followed by the TRLS method. Mixture A and mixture B having compositions corresponding to the equilibrium coexisting compositions of mixture C at T_1 were subjected to the single-step phase separation process at T_2 by T-jump from T_0 to T_2, and the TRLS experiments were performed to capture the time evolution of the LS data. All the measured scattering intensity data were corrected[13] for its fluctuation of the incident beam intensity with time, turbidity of the sample and its time change, the change in solid angle subtended by our detector with changing θ, and if necessary the background scattering caused by two cover glasses and the neat samples of dPB and hPI.[14] The corrected scattering intensity is designated by, $I_i(q,t;T)$, where subscript i indicates mixtures A, B, and C (also AB later on), and q is magnitude of the scattering vector defined by

$$q = (4\pi n/\lambda)\sin(\theta/2), \tag{1}$$

in which n is the average refractive index of the mixture.

III. RESULTS

A. LS profiles in the single-step isothermal SD at T_1 for mixture C

Figure 2 shows the time evolution of the LS profile in the single-step isothermal SD process for mixture C at T_1. The scattering maximum appeared some time after T-jump from T_0 to T_1 and the peak position, q_m, shifted towards small q with increasing its maximum intensity I_m with time, which shows a typical phase separation process of a critical binary polymer mixture.[14,15] The solid line shows the LS profile for mixture C at T_0 before the first-step phase separation.

B. LS profiles after the second-step phase separation

In Fig. 3 the time evolution of the LS profile in the second-step phase separation process for mixture C is shown. Here we define another time elapsed after the second-step T-jump as $t', t' \equiv t - t_0$. The LS profile designated as the data obtained at $t'=0$, i.e., $I_C(q,t'=0;T)$ (a solid line), actually corresponds to the LS profile obtained immediately before the second-step T-jump. It has a scattering peak at $q_m = 1.19 \times 10^{-3}$ nm^{-1}, corresponding to the characteristic length of the phase-separated structures, $\Lambda_{m,1} = 5.28\,\mu$m, where the relation $\Lambda_m = 2\pi/q_m$ was used. Immediately after the second-step T-jump, q_m shifted toward a small q and I_m increased, indicating the phase-separated structure formed during the first-step SD further grew with time. Hereafter we designate the peak as the ''first-order peak'' and the position and intensity of the first-order peak as $q_{m,1}$ and $I_{m,1}$, respectively, and the corresponding phase-separated structures as the ''large domains.'' In addition a broad peak appeared at high q and shifted toward small q with increasing its intensity as well, indicating that new composition fluctuations developed inside the large domains formed before the second-step phase separation and grew with time as described elsewhere.[4,5] We designate the peak as the ''second-order peak'' and its peak position and peak intensity as $q_{m,2}$ and $I_{m,2}$, respectively, and the corresponding composition fluctuations as the ''small domains.''

IV. ANALYSIS AND DISCUSSION

A. Initial structure existed on the second-step phase separation process

In the case of a single-step isothermal SD at T the scattering function $I(q,t;T)$ can be expressed as

$$I(q,t;T) \sim \langle \eta(t;T)^2 \rangle q_m(t;T)^{-3} S(x,t), \tag{2}$$

where $\langle \eta(t;T)^2 \rangle$ is the mean-squared composition fluctuations, $S(x,t)$ is the scaling function which depends only on the shape of the structures, and x is the reduced scattering vector defined by $x \equiv q/q_m(t;T)$. The scaled structure factor, $F(x,t;T)$, is defined as

$$F(x,t;T) \equiv q_m(t;T)^3 I(q,t;T) \sim \langle \eta(t;T)^2 \rangle S(x,t). \quad (3)$$

When the phase-separated structures grow with dynamical self-similarity in the late stage of SD, $F(x,t;T)$'s obtained at various t's fall onto a time-independent universal function with x, since the shape of the phase-separated structures at various t, related to $S(x,t)$, is statistically identical, independent of t, and the amplitude of the composition fluctuations, related to $\langle \eta(t;T)^2 \rangle$, takes a time-independent constant value determined only by T at a given pressure and for a given composition. This result is well-known as dynamical scaling hypothesis.[16]

The time evolution of the scaled structure factor for the first-step phase separation process at T_1, $F_C(x,t;T_1)$ (''C'' denotes mixture C), obtained by Eq. (3), is shown in Fig. 4. Here $F_C(x,t;T_1)$'s at various t's fall onto the universal curve characteristic of bicontinuous ''spongelike structure,''[3] which indicates when the second-step phase separation was initiated, i.e., at $t=t_0(=2865\,\text{min})$, the system had attained obviously in the late stage SD and the two phase-separated domains had the respective equilibrium coexisting compositions determined by T, i.e., T_1 here (see Fig. 1). We denote these coexisting phases as A and B, respectively.

B. General features for the early stage of the single-step isothermal SD

In general the structure evolution in the early stage of an isothermal SD at T is described according to the linearized theory by Cahn[6] or Cook.[7] According to the theory derived by Cahn:

(i) The scattered intensity grows exponentially with time as given by

$$I(q,t;T) \sim I(q,t=0;T)\exp[2R(q;T)t], \quad (4)$$

which leads to the linear relation of $\ln I(q,t;T)$ vs t,

$$\ln I(q,t;T) \sim \ln I_0 + 2R(q;T)t, \quad (5)$$

where $I_0 \equiv I(q,t=0;T)$ and $R(q;T)$ is the growth rate of q-Fourier modes of the composition fluctuations. $R(q;T)$ is given by

$$R(q;T) = D_{\text{app}}(T)q^2\{1 - q^2/[2q_m(0;T)^2]\}, \quad (6)$$

where $D_{\text{app}}(T)$ and $q_m(0;T)$ are the mutual diffusion coefficient and the wave number of the dominant mode of the composition fluctuations, respectively.

(ii) The dominant mode of the composition fluctuations has wave number q given by $q=q_m(0;T)$, for which $R(q;T)$ becomes maximum. This characteristic wave number in the early stage SD, $q_m(0;T)$, is constant with time.

C. Early stage analysis for the second-step SD process

First, let us note that $q_{m,1}$ and $I_{m,1}$, characterizing the first-order peak, have not changed much in the very early stage after the second-step T-jump, as shown in Fig. 5(a), where the time evolutions of $q_{m,1}$ and $I_{m,1}$ are plotted as a function of t'. In addition, the scattering function corresponding to the initial state (solid line), $I_C(q,t'=0;T_2)$, and that at $t'=5$ min (●) [indicated by vertical solid line in part (a), the long time limit where the linear evolution behavior of Eq. (5) was experimentally confirmed as shown by Fig. 6(a) later], $I_C(q,t'=5;T_2)$, are compared with each other in Fig. 5(b). This figure also reveals that a significant change in the scattering profile occurred in the high q range but not in the low q range during the very early stage. Therefore we do not apply any special corrections or treatments to the LS intensity distribution with q to the analysis of the early stage. In other words the scattering function $I_C(q,t'=0;T_2)$ is just the initial scattering function corresponding to $I(q,t=0;T)$ in Eq. (4) or I_0 in Eq. (5). The arrows in Fig. 5(b) indicate the low and high q limits of the q range used for the linear analysis based on Eqs. (5) and (6).

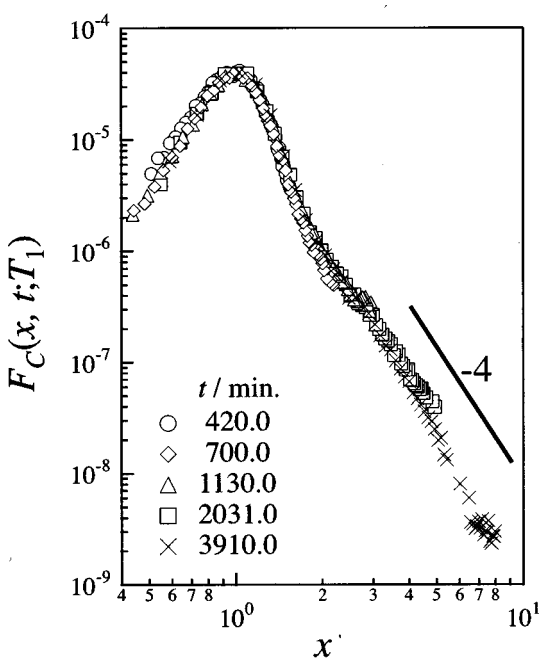

FIG. 4. Time evolution of the scaled structure factor, $F_C(x,t;T_1)$, in the late stage of the single-step isothermal SD at T_1. They fall onto the time-independent universal function as described in the text.

The analysis for the early stage in the second-step phase separation process was conducted simply according to Cahn's linearized theory described above, i.e., Eqs. (4)–(6). Figure 6(a) shows $\ln I_C(q,t';T_2)$ vs t' plots at several q's (marker symbols) and the best-fitted lines for $\ln I_C(q,t';T_2)$ vs t' (straight solid lines). Here $R_C(q;T_2)$ at each q was obtained from the slope of each fitted-line according to Eq. (5), and $R_C(q;T_2)/q^2$ was plotted against q^2 in Fig. 6(b). Note that the subscript C in $R_C(q;T_2)$ designates the data obtained for mixture C. According to Eq. (6), $D_{\text{app,C}}(T_2)$ and $q_{m,C}(0;T_2)$, corresponding to $D_{\text{app}}(T)$ and $q_m(0;T)$ for mixture C, respectively, were evaluated to be $62.9 \pm 1.1\,\text{nm}^2/\text{s}$ and $1.17 \pm 0.03 \times 10^{-2}\,\text{nm}^{-1}$, respectively (see Table III for mixture C 58.6/41.4, ''confined-SD'' process). It is obvious that the linear relation between $\ln I_C(q,t';T_2)$ and t' holds

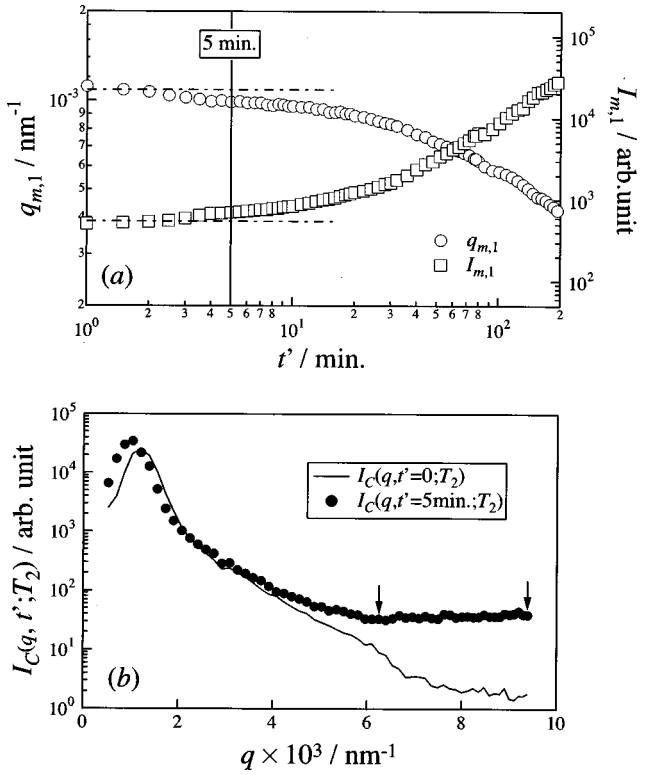

FIG. 5. (a) Time evolution of the position $q_{m,1}$ and intensity $I_{m,1}$ of the first-order peak in the second-step phase separation process. The dashed–dotted lines indicates the visual guides corresponding to the initial values of $q_{m,1}$ and intensity $I_{m,1}$ at $t'=0$. (b) Comparison between the scattering profile at $t'=0$, $I_C(q,t'=0;T_2)$ (solid lines), and that at $t'=5$ min, $I_C(q,t'=5;T_2)$ (filled circles), corresponding to the long time limit up to which the intensity data at the q-range covered in this work increase exponentially with time according to Eq. (5) in the text. The arrows indicate the low and high q limits of the q range used for the linear analysis based on Eqs. (5) and (6).

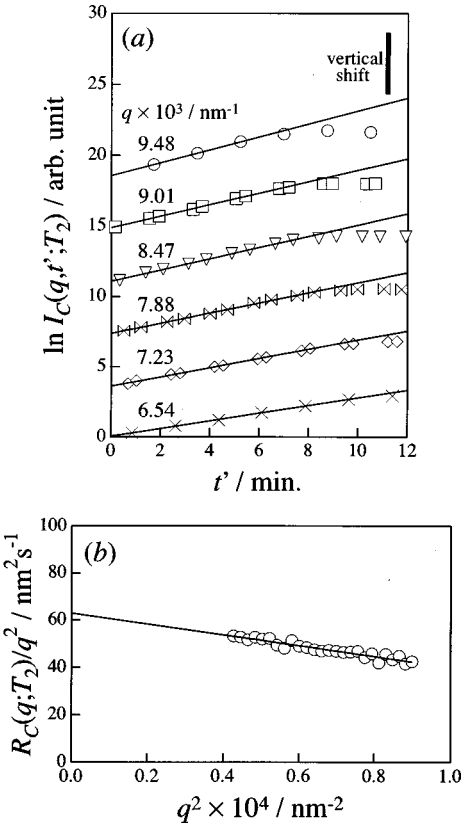

FIG. 6. Data in the early stage of the second-step phase separation process. (a) $\ln I_C(q,t';T_2)$'s at several representative q's (marker symbols) are plotted against t'. Each of them is shifted upward by factor 4 in the natural logarithmic scale (e^4) relative to the data at $q=6.54\times10^{-3}$ nm^{-1} in order to avoid overlaps of the plots. The slope of each best-fitted line (solid line) is related to the growth rate, $R_C(q;T_2)$, of the q-Fourier modes of the composition fluctuations. (b) $R_C(q;T_2)$'s are obtained from part (a) as described in the text, and $R_C(q;T_2)/q^2$ are plotted as a function of q^2. The mutual diffusion coefficient $D_{\text{app,C}}(T_2)$ and the wave number of the dominant mode of the fluctuations, $q_{m,C}(0;T_2)$, are evaluated from this plot according to the analysis based on Cahn's linearized theory.

well and $R_C(q;T_2)/q^2$ shows a good linearity against q^2, which make us convince that Cahn's linearized theory holds even in the early stage of the second-step phase separation process, as is well borne out for the single-step phase separation via SD at deep quenches for mixtures composed of high molecular weight polymers.[2]

It should also be noted that we observe a single SD peak with $q_{m,C}(0;T_2)$ rather than two SD peaks corresponding to the characteristic wave numbers $q_m(0;T_2)$ for the SD processes within the two phase-separated domains. This is simply because the SDs occurring in the two phases are very similar to each other as expected from approximately symmetrical situation of the two phases (A) and (B) at the phase separation temperature T_2. Thus broad SD peaks with nearly identical characteristic wave numbers $q_m(0;T_2)$ are overlapped each other to form a single broad SD peak.

D. Concept for superposition of the ''free-SD'' processes and the ''confined-SD'' process

Needless to say that the scattering whose time evolution follows Cahn's linearized theory is caused by the composition fluctuations newly developed inside the large domains. Since the fluctuations developed are surrounded by the interfaces of the large domains or, in other words, they are developed in the space confined by the interface of the large domains, we would denote such a SD process as ''confined-SD.'' On the contrary, we would denote the typical SD process, which is initiated in the space free from confinement as in the case of the single-step isothermal SD induced by T-jump from T_0 to T_1 or T_2, as ''free-SD.'' In this way we distinguish the single-step phase separation process and the second-step phase separation process. It is crucial to elucidate nonlinear effects about couplings between the new composition fluctuations and the space confinement.

As already mentioned, the initial structure for the second-step phase separation is the spongelike structure developed in the late stage of SD at T_1 which consists of the two phase-separated large domains having equilibrium coexisting compositions indicated by A and B in Fig. 1. It is conceivable, in principle, that the very early stage of the phase separation process involved in the two phase-separated *large domains* may be equal to an average phase separation process of the two single-step isothermal SD processes for the mixture having the respective compositions A and B as shown in parts (a) and (b) of Fig. 7. This is well expected in the context of the linearized theory of SD. As a piece of evi-

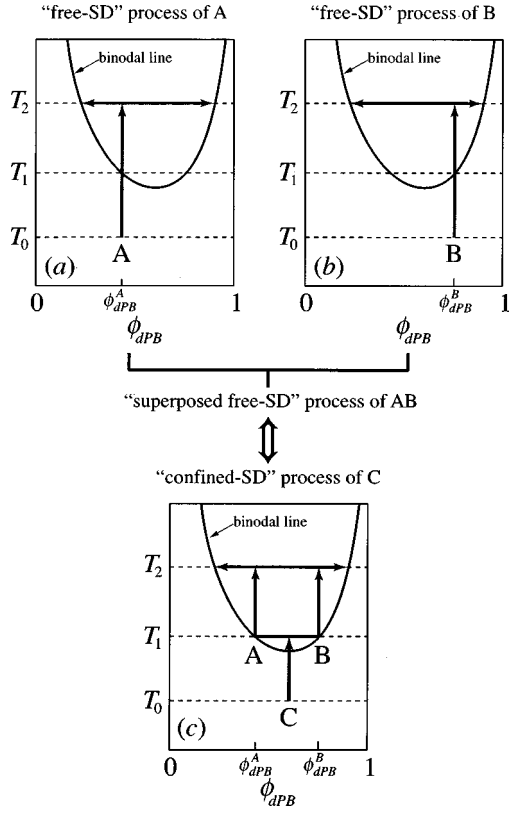

FIG. 7. Schematic presentation of (a) the single-step isothermal SD process (''free-SD'' process of A) at T_2 for mixture A having a composition $\phi^{\mathrm{A}}_{\mathrm{dPB}}$ corresponding to the equilibrium coexisting composition of mixture C at T_1, (b) the single-step isothermal SD process (''free-SD'' process of B) at T_2 for mixture B having a composition $\phi^{\mathrm{B}}_{\mathrm{dPB}}$ corresponding to the equilibrium coexisting composition of mixture C at T_1 and (c) the two-step phase separation process (the first-step SD at T_1 and ''confined-SD'' process of C at T_2) for mixture C. The early stage SD process after the second-step phase separation (''confined-SD'' process of C) was compared with the early stage SD processes for the ''free-SD'' processes of A and B as well as the early stage SD process expected for a superposition of two ''free-SD'' processes of A and B (''superposed free-SD'' process of AB).

dence supporting this concept we reported in the previous paper[5] that the characteristic size of the small domains developed at $t' \cong 0$ are approximately constant, independent of the size of the large domains existed at the onset of the second-step phase separation. In other words the characteristic wave number $q_{m,2}(0;T_2)$ for the small domains are approximately constant independent of $\Lambda_{m,1}(t'=0)$. Therefore, it may be anticipated that the time evolution of the scattering in the early stage of the second-step phase separation process (denoted as ''confined-SD'' process of C in Fig. 7 and Table III) can be expressed by a superposition of those in the early stage of the single-step isothermal SD at T_2 in mixture A (''free-SD'' process of A) and B (''free-SD'' process of B) as schematically shown in Fig. 7. This is a concept which leads us to compare ''confined-SD'' process of C and the SD process expected for a superposition of two ''free-SD'' processes of A and B (designated ''superposed free-SD'' process of AB in Fig. 7 and Table III). The concept of the ''superposed free SD'' process of AB is valid if each phase A or B undergoes SD independently each other. We shall quantitatively test validity of this concept in Sec. IV F later.

E. Early stage of the single-step isothermal SD at T_2 for mixtures A and B

Figure 8(a) shows the time evolution of the LS profile in the early stage of the single-step isothermal SD at T_2 for mixture B (''free-SD'' process of B defined in Table III and Fig. 7), where I_{B} corresponds to the scattering intensity from mixture B. Figure 8(b) indicates that the time evolutions of the scattering intensity at given q's are well described by Cahn's linearized theory here and the parameters $D_{\mathrm{app,B}}(T_2)$ and $q_{m,\mathrm{B}}(0;T_2)$ are obtained to be $23.2 \pm 1.5\,\mathrm{nm}^2/\mathrm{s}$ and $2.01 \pm 0.49 \times 10^{-2}\,\mathrm{nm}^{-1}$, respectively, from $R_{\mathrm{B}}(q;T_2)/q^2$ vs q^2 plot in Fig. 8(c) (see Table III for mixture B in the ''free-SD'' process). The identical analysis by Cahn's linearized theory was conducted for mixture A, though the results corresponding to Figs. 8(a)–8(c) were not shown here, and the characteristic parameters $D_{\mathrm{app,A}}(T_2)$ and $q_{m,\mathrm{A}}(0;T_2)$ were obtained to be $1.86 \pm 0.01 \times 10^2\,\mathrm{nm}^2/\mathrm{s}$ and $8.40 \pm 0.05 \times 10^{-3}\,\mathrm{nm}^{-1}$, respectively (see Table III for mixture A in the ''free-SD'' process).

F. ''Superposed free-SD'' process of AB and comparison of it with the ''confined-SD'' process of C

According to the discussion in Sec. IV D, the time evolution of the scattering in the second-step phase separation process (''confined-SD'' process of C), $I_{\mathrm{C}}(q,t';T_2)$, was compared with the time evolution of scattering for ''superposed free-SD'' process of AB, I_{AB}, given by a simple weighted average of $I_{\mathrm{A}}(q,t';T_2)$ and $I_{\mathrm{B}}(q,t';T_2)$ for ''free-SD'' processes of A and B, respectively,

$$I_{\mathrm{AB}} = v_{\mathrm{A}} I_{\mathrm{A}} + v_{\mathrm{B}} I_{\mathrm{B}}. \tag{7}$$

The statistical weights v_{A} and v_{B} are equal to volume fractions of coexisting two phases A and B in the late stage of the single-step isothermal SD at T_1 and are calculated to be 0.66 and 0.34 from the phase diagram shown in Fig. 1 using lever rule.

In order to make a fair comparison between $I_{\mathrm{AB}}(q,t';T_2)$ and $I_{\mathrm{C}}(q,t';T_2)$, the increment of the intensity from those in the respective initial states [i.e., $I_{\mathrm{AB}}(q;T_0)$ and $I_{\mathrm{C}}(q,t'=0;T_2)$] defined by

$$I_{\mathrm{AB},s}(q,t;T_2) \equiv I_{\mathrm{AB}}(q,t';T_2) - I_{\mathrm{AB}}(q;T_0) \tag{8}$$

and

$$I_{\mathrm{C},s}(q,t';T_2) \equiv I_{\mathrm{C}}(q,t';T_2) - I_{\mathrm{C}}(q,t'=0;T_2) \tag{9}$$

are plotted in Fig. 9, since there is a large difference between $I_{\mathrm{AB}}(q;T_0)$ and $I_{\mathrm{C}}(q,t'=0;T_2)$. In fact $I_{\mathrm{AB}}(q;T_0)$ corresponds to the scattering arising from the single-phase state at T_0 described by random phase approximation[17] and $I_{\mathrm{C}}(q,t'=0;T_2)$ to that arising from the two-phase state having q-dependence such as $I_{\mathrm{C}}(q,t'=0;T_2) \sim q^{-4}$ due to the sharp interfaces[18,19] of the large domains and to the q range covered in this study (see Fig. 4).

Looking at Fig. 9, the structure evolution of ''confined-SD'' process of C($I_{\mathrm{C},s}$) and that of ''superposed free-SD'' process of AB($I_{\mathrm{AB},s}$) are obviously not consistent with each other, which reflects the essential difference between the two cases, and hence gives a clear manifestation of intrinsically

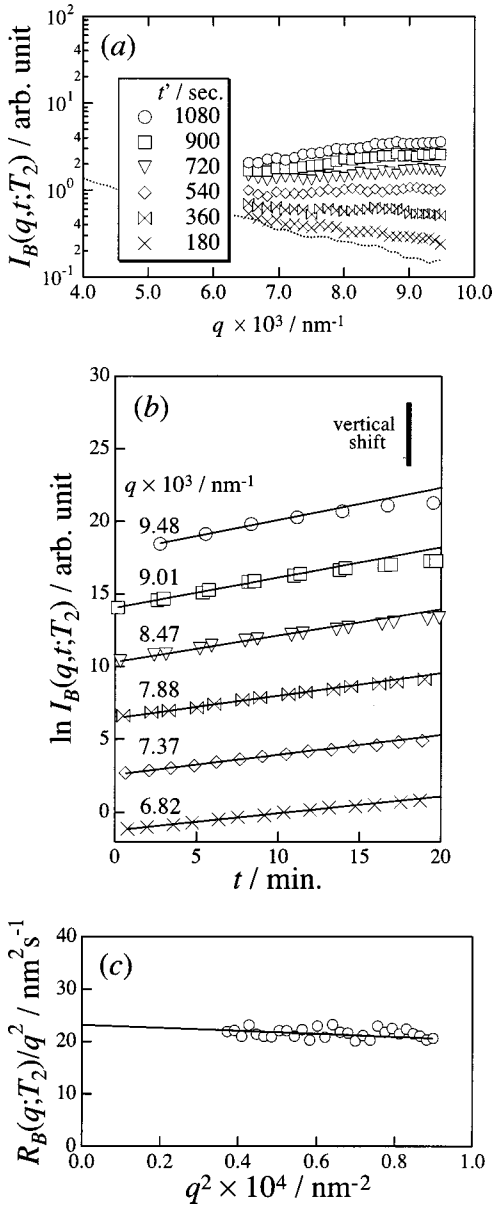

FIG. 8. Data for the early stage of the single-step isothermal SD at T_2 for mixture B. (a) Time evolution of the light scattering profile during the early stage of SD at T_2. (b) $\ln I_B(q;t;T_2)$'s at several representative q's (marker symbols) are plotted against t. Each of them is shifted upward by factor 4 in the natural logarithmic scale (e^4) relative to the data at $q=6.82\times10^{-3}$ nm^{-1} in order to avoid overlaps of the plots. The slope of each best-fitted line (solid line) is related to the growth rate, $R_B(q;T_2)$, of the q-Fourier modes of the fluctuations. (c) $R_B(q;T_2)$'s are obtained from part (b) as described in the text, and $R_B(q;T_2)/q^2$ are plotted as a function of q^2. $D_{app,B}(T_2)$ and $q_{m,B}(0;T_2)$ can be evaluated from this plot according to the analysis based on Cahn's linearized theory.

nonlinear phenomenon, because the growth of the composition fluctuations in the early stage is affected by the space confinement and the growth in phase A and that in phase B are not independent each other. The early stage of ''superposed free-SD'' process of AB is further analyzed below.

G. Early stage of the ''superposed free-SD'' process of AB

The early stage of the ''superposed free-SD'' process of AB was explored according to Cahn's linearized theory in the same way as already described. Figures 10(a) and 10(b) show $\ln I_{AB}(q,t';T_2)$ vs t' and $R_{AB}(q;T_2)/q^2$ vs q^2 plots, respectively, which reveal that the linearized theory also holds well for the ''superposed free-SD'' process of AB. The values for $D_{app,AB}(T_2)$ and $q_{m,AB}(0;T_2)$ were estimated to be $1.60\pm0.01\times10^2$ nm^2/s and $9.13\pm0.05\times10^{-3}$ nm^{-1}, respectively (see Table III for the ''superposed free-SD'' process of AB). Again we observe a single SD peak with $q_{m,AB}(0;T_2)$ for the ''superposed free-SD'' process of AB simply because SD peaks from A and B are very broad and have nearly identical characteristic wave numbers $q_{m,A}(0;T_2)\cong q_{m,B}(0;T_2)$ as clearly manifested in Table III and hence the two broad peaks are overlapped in a single broad peak.

TABLE III. Parameters for the early stages.

Mixture code	dPB/hPI (vol%/vol%)	$D_{app,i}(T_2)$ (nm^2/s)	$q_{m,i}(0;T_2)$ (nm^{-1})	$\Lambda_{m,i}(0;T_2)$[a] (nm)
''Confined-SD'' process				
C	58.6/41.4	$6.29\pm0.11\times10^1$	$1.17\pm0.03\times10^{-2}$	536 ± 14
''Superposed free-SD'' process				
AB	···	$1.60\pm0.01\times10^2$	$9.13\pm0.05\times10^{-3}$	688 ± 4
''Free-SD'' process				
A	50.2/49.8	$1.86\pm0.01\times10^2$	$8.40\pm0.05\times10^{-3}$	748 ± 4
B	75.2/24.8	$2.32\pm0.15\times10^1$	$2.01\pm0.49\times10^{-2}$	332 ± 80

[a] $\Lambda_{m,i}(0;T_2)\equiv2\pi/q_{m,i}(0;T_2)$ with i=C, AB, A or B.

Seeing Table III, the difference among ''confined-SD'' process of C, ''superposed free-SD'' process of AB, ''free-SD'' process of A, and ''free-SD'' process of B is remarkable in the value of $D_{app,i}(T_2)$. For example $D_{app,C}(T_2)$ is about one-half of $D_{app,AB}(T_2)$, whereas $q_{m,AB}(0;T_2)$, $q_{m,A}(0;T_2)$, $q_{m,B}(0;T_2)$, and $q_{m,C}(0;T_2)$ are almost equal to each other.

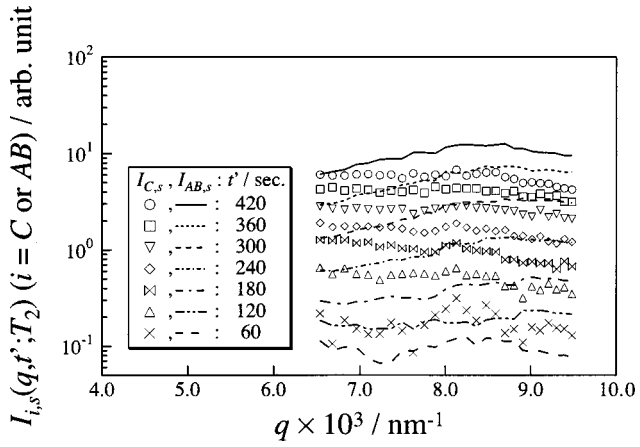

FIG. 9. Comparison between the time evolution of the light scattering profile, $I_{C,s}(q,t';T_2)$, in the early stage of the second-step phase separation process (''confined-SD'' process of C) and that of the scattering profile, $I_{AB,s}(q,t';T_2)$, calculated by a superposition of the scattering profiles for the two ''free-SD'' processes of A and B at T_2 (''superposed free-SD'' process of AB), where the respective scattering intensity distributions are subtracted by the scattering at $t'=0$, $I_C(q,t'=0;T_2)$ and by the scattering at $t=0$, $I_{AB}(q;T_0)$, respectively.

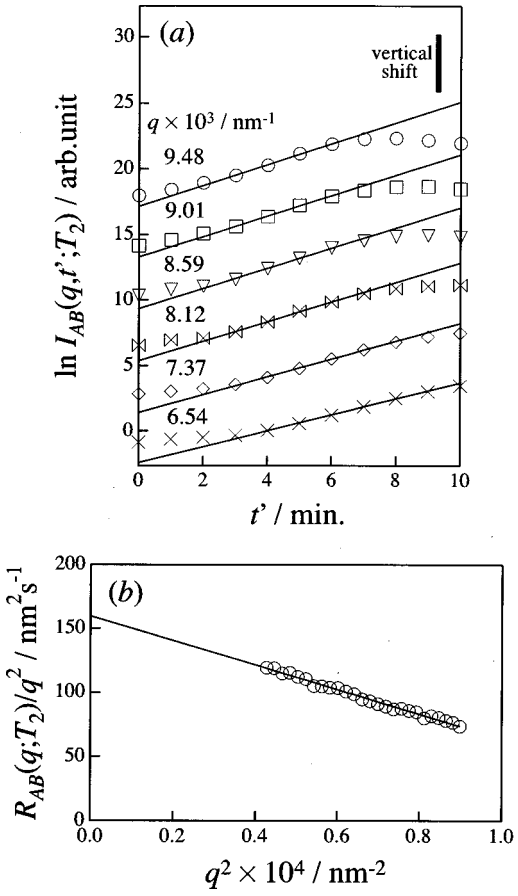

FIG. 10. Time evolution of $I_{AB}(q,t';T_2)$ for the ''superposed free-SD'' process of AB. (a) $\ln I_{AB}(q,t';T_2)$'s at several representative q's (marker symbols) are plotted against t'. Each of them is shifted upward by factor 4 in the natural logarithmic scale (e^4) relative to the data at $q=6.54 \times 10^{-3}$ nm^{-1} in order to avoid overlaps of the plots. The slope of each best-fitted line (solid line) is related to the growth rate, $R_{AB}(q;T_2)$, of the q-Fourier modes of the fluctuations. (b) $R_{AB}(q;T_2)$'s are obtained from part (a) as described in the text, and $R_{AB}(q;T_2)/q^2$ are plotted as a function of q^2. The mutual diffusion coefficient $D_{app,AB}(T_2)$ and the characteristic wave number $q_{m,AB}(0;T_2)$ for the dominant modes of the fluctuations can be evaluated from this plot according to the analysis based on Cahn's linearized theory. Note that $I_{AB}(q,t';T_2)$ was not corrected for $I_{AB}(q;T_0)$ as in the case of $I_i(q,t';T_2)$ (i=A, B, or C).

H. Effects of space confinement on the time evolution of the composition fluctuations

According to the results in the previous section, the effect of space confinement on the time evolution of the composition fluctuations remarkably manifest itself on the mutual diffusion coefficient $D_{app,i}(T_2)$ but not on the characteristic wave number $q_{m,i}(0;T_2)$ of the dominant modes of the fluctuations (see Table III). These features may be understood as follows. The initial characteristic size of the large domains, 5 μm, is large enough compared with the characteristic length $[\Lambda_{m,C}(0;T_2)=0.536\pm0.014\,\mu\text{m}]$ of the dominant modes of the new composition fluctuations (see last column in Table III). Further the initial size of the small domains grown from the composition fluctuations inside the large domains are almost independent of the size of the large domains as reported in the previous paper.[5] These two pieces of experimental evidence may elucidate that the initial size of the small domains are not spatially affected as long as there is enough space $[\Lambda_{m,1}(t'=0)\geqslant 1.5\,\mu\text{m}]$ for them to be generated. On the other hand, as for the growth rate $R(q;T_2)$ for the q-Fourier modes of the composition fluctuations, the growth rate will be coupled with the interface of the large domains and should be slowed down compared with the growth rate in the free-SD process. This is because newly excited Fourier modes of the composition fluctuations in the large domains rich in A, for example, may be able to grow further when they satisfy the boundary condition brought by the interfaces with the large domains, rich in B. The smaller the q value, the larger the coupling and hence the larger the suppression of the growth rate. The difference between $D_{app,C}(T_2)$ and $D_{app,AB}(T_2)$ may be interpreted this way.

V. CONCLUDING REMARKS

We explored an early stage spinodal decomposition (SD) process started from a well characterized two-phase coexisting structure as an initial structure, based on the linearized theory of SD. In order to explore this unique SD, we used a model binary mixture of dPB and hPI having a composition close to critical composition and imposed a two-step phase separation to this mixture as shown in Fig. 1. In the first-step phase separation via SD at temperature $T_1(=42\,^\circ\text{C})$, we brought our mixture from a single phase at temperature T_0 (=room temperature) into a late stage of SD at T_1 so that the two coexisting phases A and B (as defined in Fig. 1) build up a bicontinuous structure characteristic of the ''spongelike structures'' with a characteristic size $\Lambda_{m,1}=5.28\,\mu$m and equilibrium compositions $\phi^{\text{A}}_{\text{dPB}}$ and $\phi^{\text{B}}_{\text{dPB}}$. We then brought the system in the second-step phase separation at temperature $T_2(=70\,^\circ\text{C})$ by rapidly changing temperature from T_1 to T_2 where the coexisting phases A and B were again exposed to thermodynamic instability and thereby created new composition fluctuations leading to formation of small domains within each coexisting phase in a later time in the phase separation process.

We explored a very early stage of this spinodal SD process, by means of time-resolved light scattering (TRLS), over the time domain of which the pre-existed two phases hardly changed with time and thus provided a sort of ''confined space'' for the new SD process. This SD process in confined space (denoted ''confined-SD'' process of C in the text) was compared with the corresponding SD processes in free space (denoted ''free-SD'' process of A and ''free-SD'' process of B, respectively, i.e., the single-step SD process of the mixtures having their compositions equal to the coexisting phases A and B brought by a temperature jump from T_0 to T_2) (see an illustration shown in Fig. 7). This ''confined-SD'' process of C was also compared with ''superposed free-SD'' process of AB defined as the SD process expected for a superposition of ''free-SD'' processes of A and B with a proper statistical weight discussed in the text.

First of all, ''confined-SD'' process of C, ''free-SD'' process of A and B, and ''superposed free-SD'' process of AB studied in this work are found to be well characterized by the linearized theory of SD, in consistent with the earlier results on high molecular weight polymer mixtures in deep quenches.[15,20] In second, as summarized in Table III, the

result clearly elucidated that the characteristic parameters describing the early stage SD [mutual diffusivity $D_{\mathrm{app},i}(T_2)$ and the characteristic wave number $q_{m,i}(0;T_2)$ ($i=$A, B, AB, or C)] obtained for ''confined-SD'' process of C are different from those obtained for ''free-SD'' processes of A and B and from those obtained for ''superposed free-SD'' process of AB.

Both $D_{\mathrm{app,C}}(T_2)$ and $q_{m,\mathrm{C}}(0;T_2)$ for the ''confined-SD'' process of C are in between those for the corresponding ''free-SD'' process of A and the ''free-SD'' process of B and these values are qualitatively identical. In this qualitative level, the results are consistent with the theoretical prediction and hence the linear theory works well. However if we compare $D_{\mathrm{app,C}}(T_2)$ and $q_{m,\mathrm{C}}(0;T_2)$ for the ''confined-SD'' process of C with $D_{\mathrm{app,AB}}(T_2)$ and $q_{m,\mathrm{AB}}(0;T_2)$ for the ''superposed free-SD'' process of AB, we note that $D_{\mathrm{app,C}}(T_2)$ is only about one-half of $D_{\mathrm{app,AB}}(T_2)$, though the value $q_{m,\mathrm{C}}(0;T_2)$ for the two cases happen to be approximately equal. The discrepancy in the diffusivity reflects the confined space effect on the early stage SD process and hence illuminates the intrinsically nonlinear nature of this time evolution process. The space confinement effects are more clearly and directly clarified from the discrepancy in the time evolution of LS profiles for the ''confined-SD'' process of C from that for ''superposed free-SD'' process of AB, as shown in Fig. 9.

The space confinement effects of the SD process may be interpreted in terms of a coupling of Fourier modes of composition fluctuations with pre-existing domains. The evolution of the low q-modes of our interest here as observed by TRLS may tend to be coupled and be suppressed more strongly than that of the high q-modes, as detailed in the text. This may account for the observed discrepancy. The characteristic initial structure of size $\Lambda_{m,1}(t_0)$ existed immediately before the second-step phase separation is approximately 10 times larger than $\Lambda_{m,\mathrm{C}}(0;T_2)=2\pi/q_{m,\mathrm{C}}(0;T_2)=0.536\pm0.014\,\mu$m (see Table III). Upon decreasing $\Lambda_{m,1}(t_0)$, we expect increasing coupling effects, which would further suppress the SD process in the second-step phase separation. The effects may eventually lead us to such an earlier finding by us as we could not observe formation of the small domains when $\Lambda_{m,1}(t_0)$ was decreased to $\sim1.0\,\mu$m. In order to confirm this trend, we must detect the higher q modes developed within the large domains having smaller size than $\Lambda_{m,1}(t_0)=5.28\,\mu$m. For this purpose TRLS becomes inappropriate and we should rely on time-resolved small-angle neutron scattering. It may be also very intriguing to study this trend by computer simulations. This kind of work deserves future studies.

ACKNOWLEDGMENT

We would like to thank Professor H. Hasegawa for the synthesis of the polymers used in this study.

[1] J. D. Gunton, M. San Miguel, and P. P. Sahni, *Phase Transition and Critical Phenomena*, edited by C. Domb and J. L. Lebowitz (Academic, New York, 1983), Vol. 8, p. 269.
[2] T. Hashimoto, Phase Transit. **12**, 47 (1988); T. Hashimoto, in *Materials Science and Technology*, edited by R. W. Cahn, P. Haasen, and E. J. Kramer, Vol. 12 in *Structure and Properties of Polymers*, edited by E. L. Thomas (VCH, Weinheim, 1993), Chap. 6.
[3] T. Hashimoto, H. Jinnai, Y. Nishikawa, T. Koga, and M. Takenaka, Prog. Colloid Polym. Sci. **106**, 118 (1997); T. Hashimoto, T. Koga, H. Jinnai, and Y. Nishikawa, Nuovo Cimento D **20**, 1947 (1998).
[4] T. Hashimoto, M. Hayashi, and H. Jinnai, J. Chem. Phys. **112**, 6886 (2000).
[5] M. Hayashi, H. Jinnai, and H. Hashimoto, J. Chem. Phys. **112**, 6897 (2000).
[6] J. W. Cahn, J. Chem. Phys. **42**, 93 (1965).
[7] H. E. Cook, Acta Metall. **18**, 287 (1970).
[8] M. Okada, K. D. Kwak, T. Chiba, and T. Nose, Macromolecules **26**, 4047 (1993).
[9] H. Tanaka, Phys. Rev. E **47**, 2946 (1993).
[10] J. Tao, M. Okada, T. Nose, and T. Chiba, Polymer **36**, 3919 (1995).
[11] T. Hashimoto, J. Kumaki, and H. Kawai, Macromolecules **16**, 641 (1983).
[12] P. J. Flory, *Principles of Polymer Chemistry* (Cornell University, Ithaca, 1971).
[13] R. S. Stein, and J. Keane, J. Chem. Phys. **17**, 21 (1955).
[14] M. Takenaka and T. Hashimoto, J. Chem. Phys. **96**, 6177 (1992).
[15] T. Hashimoto, M. Itakura, and H. Hasagawa, J. Chem. Phys. **85**, 6118 (1986).
[16] K. Binder and D. Stauffer, Phys. Rev. Lett. **33**, 1006 (1974); K. Binder, Phys. Rev. B **15**, 4425 (1977).
[17] P. G. de Gennes, *Scaling Concepts in Polymer Physics* (Cornell University, Ithaca, 1979).
[18] G. Porod, Kolloid-Z. **124**, 83 (1951); **125**, 51 (1952).
[19] J. S. Higgins and H. C. Benoit, *Polymers and Neutron Scattering* (Oxford University Press, New York, 1994), pp. 236 and 786.
[20] M. Takenaka, T. Hashimoto, and T. Izumitani, Macromolecules **20**, 2257 (1987).